

# The design of the IRIS inelastic neutron spectrometer and improvements to its analysers

C.J. Carlile and M.A. Adams

ISIS Pulsed Source, Rutherford Appleton Laboratory, Chilton, Didcot, UK

The design principles of the IRIS high-resolution inverted-geometry spectrometer on the ISIS pulsed source are described and the performance in terms of energy transfer and resolution derived. Recent improvements to the crystal analysers are described, notably the effect of cooling the graphite to 25 K. Future plans are indicated.

## 1. Introduction

Crystal analyser spectrometers have a fundamental advantage over direct-geometry spectrometers because of the opposite-handedness of the  $(Q, \omega)$  locii as shown in fig. 1. This means that, when studying cold samples in their excitational ground state, the neutron energy-loss technique can still be employed, giving access to large energy and momentum transfer ranges, yet maintaining the instrumental resolution. The resolution can thus be partially decoupled from the energy transfer and the final analysed neutron energy can be very low if high resolution is required. Since neutrons of the analyser energy need not be present with any intensity in the incident beam the development of synthetic long wavelength analysers, such as Langmuir Blodgett films, with  $d$ -spacings beyond that of natural crystalline materials, could even be considered in the future.

A disadvantage of the inverted-geometry technique however is that the full white beam travels into the spectrometer and falls onto the sample and its environment. This generates a neutron population within the analyser tank which is, perhaps, a hundred times higher than on a similar performance direct-geometry spectrometer.

Correspondence to: C.J. Carlile, ISIS Pulsed Source, Rutherford Appleton Laboratory, Chilton, Didcot, Oxfordshire OX11 0QX, UK.

The effect becomes more severe the higher the ratio of energy transfer range to resolution width. The problem can in fact be overcome despite pessimism expressed in an early IAEA panel meeting in 1969 [1]:

H.A. Mook: "Perhaps you could use a time-of-flight spectrometer with the flight path first, then use a crystal to analyse the neutrons...";

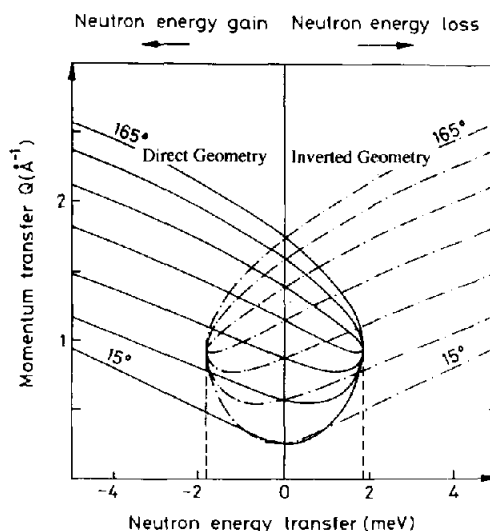


Fig. 1. The  $(Q, \omega)$ -space available to a direct-geometry and an indirect-geometry neutron scattering instrument for the same fixed energy of 1.8 meV.

B.N. Brockhouse: "I think it would be very difficult to work in the main beam with a single crystal analyser...";

G. Dolling: "It should be pointed out that you really are making things hard for yourself when you put your specimen in the main beam".

However, white-beam techniques do mean that collimation of the incident and scattered beams must be very effective and that internal shielding must be well-defined and universal. It is crucial that the crystal used as the analyser must have a very high contrast for the desired-energy neutrons compared with other energies in the incident beam. In practice this means that the ratio of the coherent elastic scattering cross section to the sum of the coherent inelastic and incoherent elastic and inelastic scattering cross sections must be very high.

The design concept of the high-resolution inelastic spectrometer IRIS came about in discussions between R. Scherm, J.S. Higgins and C.J. Carlile [2] at ILL in 1976 at a time when plans were being formulated for a high-intensity pulsed neutron source to be built at the Rutherford Appleton Laboratory in England. In due course the pulsed source, ISIS, produced its first neutrons in December 1984 and the IRIS spectrometer recorded its first spectrum in August 1988 – a gestation period for the instrument of twelve years!

The original 1976 conceptual design of IRIS included arrays of both graphite and silicon in exact backscattering geometry at the end of a 44 m long curved neutron guide viewing a liquid hydrogen moderator and having an estimated elastic resolution of 12  $\mu\text{eV}$  and 1  $\mu\text{eV}$ . IRIS was to be the pulsed-source analogue of IN10 the 1  $\mu\text{eV}$  resolution silicon-analyser backscattering spectrometer at ILL.

The spectrometer which was eventually built in 1988 dispensed with the silicon analyser for intensity reasons which then allowed the graphite-analyser array to be designed slightly off backscattering and removed the need for a beam modulation chopper before the sample.

Because of financial limits the solid angle of graphite actually installed was less than 40% of that originally specified. The distance to the sample was also reduced somewhat to  $\sim 36.5$  metres to allow the spectrometer to be housed in an extension to the main experimental hall rather than in a more costly self-contained building. As a consequence the actual resolution of the spectrometer was relaxed to 15  $\mu\text{eV}$ .

During the first three years of operation of ISIS a very valuable contribution to the eventual realisation of IRIS was made by the provision of a pair of double beryllium analysers by the Bhabha Research Centre in Bombay at the initiative of B.A. Dasannacharya. These were installed at the end of the IRIS curved guide [3].

## 2. The basic design of IRIS

For an inverted-geometry spectrometer using crystal analysers in near-backscattering geometry, the energy resolution  $\Delta E$  is represented as a convolution of three contributions,

$$\Delta E \approx 2E \left[ \frac{\Delta t_{\text{mod}}}{t} \right] * \left[ \frac{\Delta d}{d} \right] * [\cot \theta \cdot \Delta \theta],$$

where  $t$  is the total time of flight from the moderator to the detector,  $\Delta d/d$  is the uncertainty of lattice spacing of the analyser crystal and  $\Delta \theta$  is the overall uncertainty in Bragg angle at the analyzer. The first term arises from the moderator pulse width  $\Delta t_{\text{mod}}$  at a given neutron energy  $E$  and the remaining terms represent the uncertainty in lattice parameter of the analysers and the uncertainty in the definition of the Bragg angle  $\theta$  because of beam divergence and analyser mosaicity. In the case of *exact* backscattering this final term is zero.

The liquid-hydrogen moderator on ISIS generates a pulse with a width of  $22\lambda$  ( $\text{\AA}$ )  $\mu\text{s}$  at wavelengths near the peak of the Maxwellian. At longer wavelengths the width remains approximately constant at  $\sim 120 \mu\text{s}$ . Pyrolytic graphite has an uncertainty in its lattice parameter  $\Delta d/d$  of approximately  $2 \times 10^{-3}$  and the wavelength reflected from the (002) planes is 6.69  $\text{\AA}$ . Therefore, in order to match the primary resolution to the secondary resolution with the analyser in

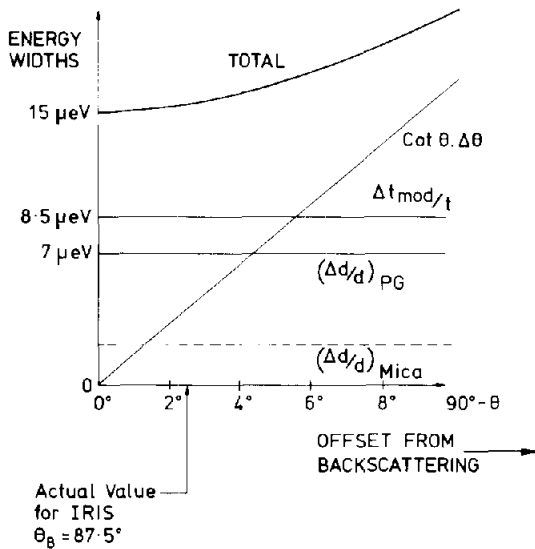


Fig. 2. The resolution components of a pulsed-source backscattering spectrometer as a function of offset from  $\theta_B = 90^\circ$  for the graphite(002) Bragg reflection. The equivalent value for mica(006) is shown as a dotted line.

exact backscattering, the primary flight path of the spectrometer must be set at around 44 metres in length. As can be seen from fig. 2, showing the components of the resolution, the  $\cot \theta \cdot \Delta \theta$  term was able to be relaxed without spoiling the overall resolution significantly. Matching of the primary resolution to the total secondary resolution occurs at a Bragg angle of  $87.5^\circ$ , both components having widths of approximately  $8.5 \mu\text{eV}$ . Since the moderator pulse shape is asymmetric, describable by a gaussian convoluted with a decaying exponential function, and the secondary resolution is approximately gaussian, the primary and secondary widths are approximately linearly additive, giving a final total resolution width of  $15.2 \mu\text{eV}$  as shown in fig. 2. A second broader gaussian component is required to account for the wings at the base of the resolution function.

### 3. Details of the spectrometer design

The liquid hydrogen moderator is viewed at an angle of  $13^\circ$  to the normal by a nickel-plated curved neutron guide which starts at 1.7 metres

from the moderator. The guide solid angle of acceptance is matched to the moderator face area for  $9 \text{ \AA}$  neutrons. It is fully illuminated at all wavelengths lower than this value. The initial two sections, inside the shutter and the target station shielding are made from highly polished steel substrates because of the intense radiation field in which they sit. The remainder of the guide is made from plate glass sections 1 metre long and of cross-section  $65 \text{ mm} \times 43 \text{ mm}$ . The radius of curvature of the guide is 2.35 km giving a characteristic wavelength  $\lambda^*$  of  $2.5 \text{ \AA}$ . In practice the neutron transmission only falls to zero at a wavelength near to  $1 \text{ \AA}$  as shown in fig. 3. The final component of the guide system is a 2.5 m long, single-section, nickel-titanium supermirror, doubly converging guide which brings the

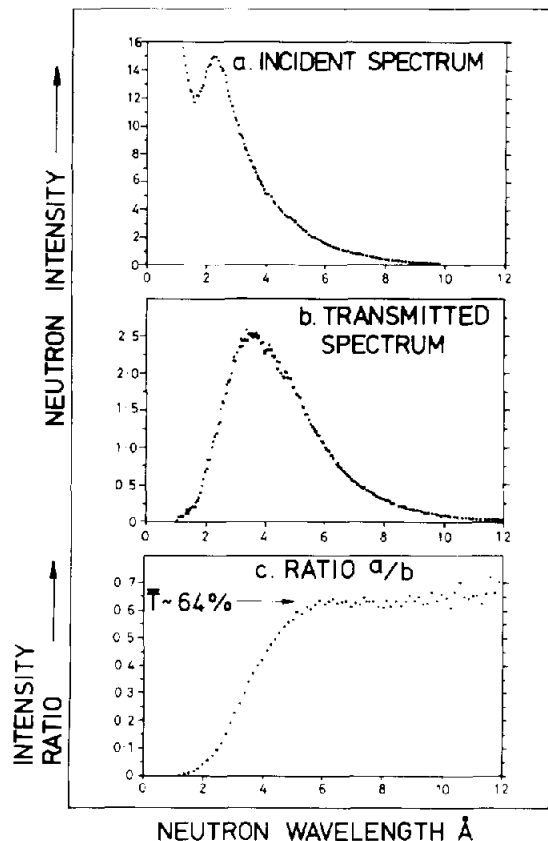


Fig. 3. The spectrum of neutrons at the entrance (a) and exit (b), as indicated in fig. 4, of the curved section of the IRIS guide and (c) a derived throughput of the guide as a function of wavelength.

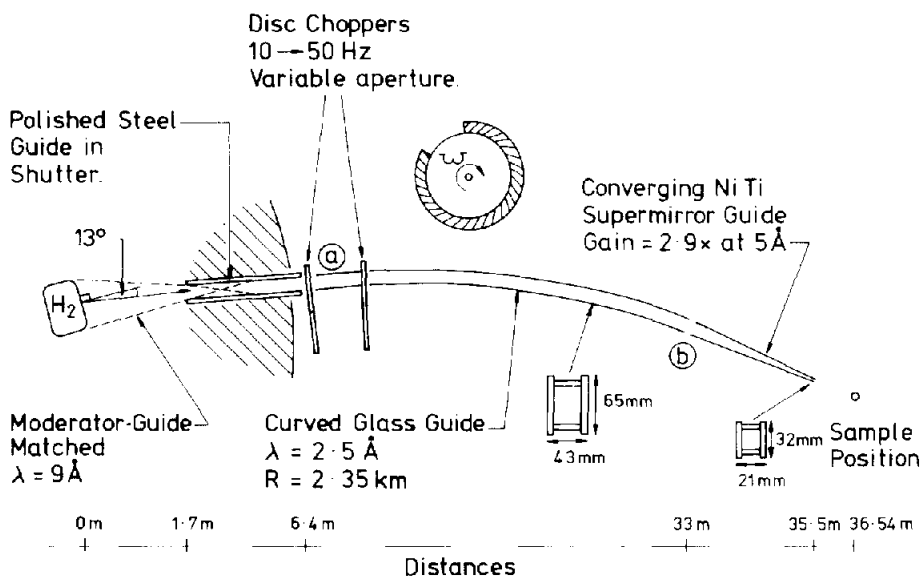


Fig. 4. The layout of the IRIS guide system from the liquid-hydrogen moderator to the sample at 36.54 m.

beam area down to 32 mm × 21 mm giving a gain in flux of a factor 2.9 at 5 Å. The guide geometry is shown in fig. 4.

In order to eliminate frame overlap at the sample position two disk choppers are located directly outside the target station at 6.4 m and 10.0 m from the moderator. The choppers normally run at 50 Hz, with variable apertures set slightly less than 60° and 100° respectively. At these settings a wavelength band of 2 Å can be delivered to the sample which sits at 36.54 m from the moderator. This wavelength band provides an energy transfer range for the pyrolytic graphite(002) reflection of ±0.4 meV. When required a wider window can be selected by running the chopper at an integral fraction of the ISIS frequency, i.e. 25 Hz, 16.7 Hz, 12.5 Hz or 10 Hz and eliminating 1 in 2, 2 in 3, 3 in 4 or 4 in 5 ISIS pulses respectively.

The IRIS analyser tank is a two-metre diameter stainless-steel vacuum vessel as shown in fig. 5. The beam monitor sits immediately after the end of the supermirror converging guide, 37 cm before the sample position. The graphite analyser sits in the horizontal scattering plane covering scattering angles from 15° to 165°, 85 cm from the sample. The analyser comprises 1350 graphite pieces each of area 1 cm<sup>2</sup> with mosaic

spread 0.8° mounted on a spherically machined aluminium backing plate. The analysed beam is scattered back to the detector through an angle of 175°, below the horizontal plane. The detector is approximately 60 cm from the analyser.

The detector is a 51-element ZnS directly coupled scintillator detector operating in 'walking coincidence'. Its gamma sensitivity and random electronic noise are well below background levels from other sources.

On the opposite side of the sample, in approximately the same geometry but with three times the area of the graphite, a mica analyser has recently been installed. Mica has a lattice parameter which is three times greater than graphite and provides higher absolute resolutions at the longer neutron wavelengths selected. It also utilises a 51-element scintillator detector giving a total of 102 detectors on the instrument.

Between the sample and the graphite analyser is a 25 K beryllium filter which renders the analyser insensitive to neutron wavelengths other than that from the (002) reflection. This allows energy transfers up to the limit of the transmission of the guide (~10 meV) to be observed. When high-*Q* quasielastic data is needed this filter can be retracted and replaced by a radial collimator.

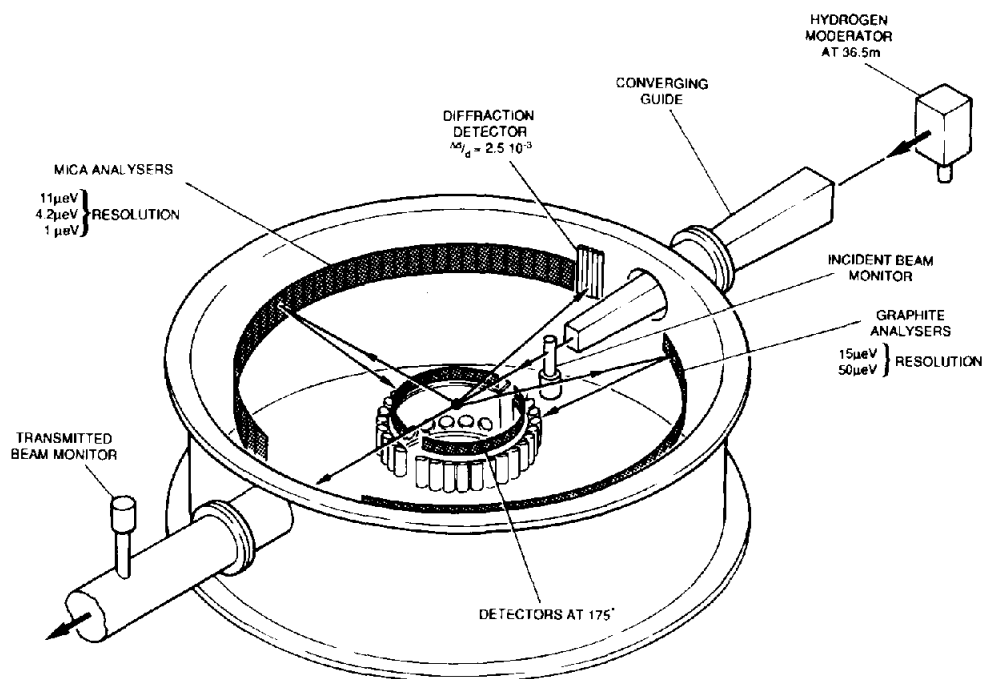


Fig. 5. The IRIS analyser vacuum vessel showing the graphite and mica analyser–detector arrays and the diffraction detectors.

A significant bonus on white-beam crystal-analyser instruments is that a diffraction pattern of the sample can be recorded simultaneously with the inelastic spectrum. This aids the diagnosis of structural phases when studying complex materials with multiple phase transitions, and hysteresis effects such as are displayed by liquid crystals. It also allows structural parameters to be linked to spectroscopic observations in the study of samples uniquely prepared in beam such

as intercalates, or those samples which are undergoing transformations in time. The IRIS diffraction detector, ten high-pressure  $\text{He}^3$  tubes, sits at a scattering angle of approximately  $175^\circ$ . It provides an almost constant resolution in  $\Delta d/d$  of  $2.5 \times 10^{-3}$  over  $d$ -spacings from  $1 \text{ \AA}$  to  $12 \text{ \AA}$  using neutrons out to wavelengths of  $25 \text{ \AA}$ .

The analyser tank is shown diagrammatically in fig. 5 and the performance characteristics of the instrument are given in table 1.

Table 1  
The performance of the IRIS inelastic spectrometer.

Analyser reflection	Analyser wavelength [ $\text{\AA}$ ]	Analyser energy [meV]	Energy resolution [ $\mu\text{eV}$ ]	Energy and momentum transfer ranges
Mica(002)	19.8	0.208	1.1	$-100 \mu\text{eV}$ to $+300 \mu\text{eV}$ $0.1$ to $0.6 \text{ \AA}^{-1}$
Mica(004)	9.9	0.832	4.2	$-400 \mu\text{eV}$ to $+500 \mu\text{eV}$ $0.2$ to $1.2 \text{ \AA}^{-1}$
Mica(006)	6.6	1.87	11	$-0.5 \text{ meV}$ to $+1 \text{ meV}$ $0.3$ to $1.8 \text{ \AA}^{-1}$
Graphite(002)	6.7	1.82	15	$-0.8 \text{ meV}$ to $+2.2 \text{ meV}$ $0.3$ to $1.8 \text{ \AA}^{-1}$
Graphite(004)	3.35	7.28	50	$-3 \text{ meV}$ to $+5 \text{ meV}$ $0.5$ to $3.7 \text{ \AA}^{-1}$

#### 4. Improvements to the analysers

##### 4.1. Increase in area

The IRIS graphite analyser as presently installed intercepts only 1.5% of the scattered beam. There is thus great scope to improve the count rate of the instrument simply by increasing the analyser area. Given that the detector must occupy an equal solid angle to the analyser and that realistic access is required by the sample environment equipment and for the passage of the incident beam through the spectrometer we are still left with 30% of the scattered solid angle in which to install analysers. A possible gain of a factor 20 is attainable if the theoretically available area were to be filled!

For *exact* backscattering no problem is encountered geometrically in increasing the analyser size since the analyser itself is then mounted on a spherical surface and can be extended without causing any optical aberration of the focus. This advantage is counterbalanced, firstly by the need for the scattered neutrons to pass

through the sample a second time, and secondly by the need for a beam modulation chopper before the sample to enable discrimination of neutrons scattered directly into the detector. The beam modulation chopper reduces the neutron flux on the sample by a factor of 2.5.

When the detector is taken off backscattering conditions, the effects of optical aberration introduce themselves. This appears as either a wavelength variation of the analysed neutrons or a path-length difference between sample and detector from various points on the analyser surface. The two possible geometries, both of which introduce a time-of-flight spread at the detector, are shown in fig. 6. The former arrangement shows the analysers set on a Rowland circle passing through the sample and the detector focal point. Since the included angle at the analyser is constant in this geometry the reflected neutron wavelength is also constant provided that the normal to the reflecting planes is directed along the bisector of the included angle. As the analyser position moves out of the horizontal scattering plane however the flight

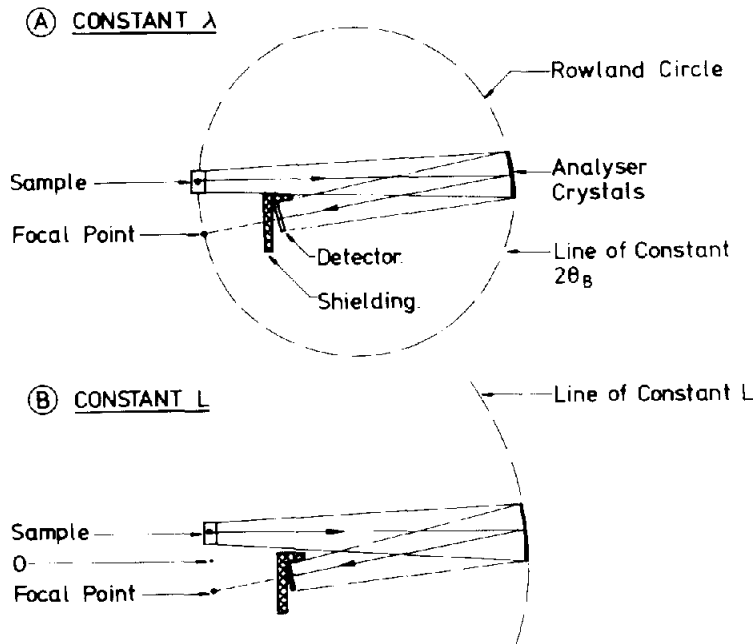


Fig. 6. The two geometrical options for setting the analysers in a near-backscattering geometry, one providing constant wavelength and the other constant flight path length.

path between sample and detector varies, resulting in a time-of-flight defocusing. The latter geometry, in which the analysers sit on a circle centred on the mid-point between the sample and detector foci, results in a negligible flight path difference as the analyzer moves out of the scattering plane, but instead the Bragg wavelength varies. In practice the second geometry is more accurate and causes less optical aberration for geometries near to backscattering. Using a combination of the two geometries numerically generated, an extension out of the horizontal plane by 20 cm can be tolerated without considerably affecting the elastic resolution, thus resulting in a gain factor greater than three in the solid angle intercepted. This has now been done by installing a large-area mica analyser.

#### 4.2. Cooling the analysers

The resolution function for the graphite analyser cannot be fitted adequately by a single gaussian convoluted with a decaying exponential but instead requires a second broadened gaussian component to be *added* to the convolution.

This additional component is due to inelastic thermal diffuse scattering (TDS) from graphite. The origin of this effect is illustrated in fig. 7 where the scattered spectrum from a pyrolytic graphite analyser illuminated by a white beam is shown as a function of angular offset from the Bragg condition. These patterns were recorded in the IRIS diffraction detector with a graphite crystal at the sample position. As the crystal is turned off the Bragg condition the TDS at the base of the intense diffraction line splits into two distinct 'wings' representing phonon creation and phonon annihilation as first observed by Carlile and Willis [4].

It is the sum of these patterns from a wide angular range of analysers which is recorded in a single detector on the spectrometer which results in the broad underlying feature centred on the elastic line, the latter (Bragg line) being reflected from a restricted analyser area. The underlying TDS has a maximum intensity approximately 1% of the elastic peak height. The integrated intensity in the TDS signal however approaches that of the elastic line itself. One method of reducing the off-Bragg TDS intensity is to introduce a

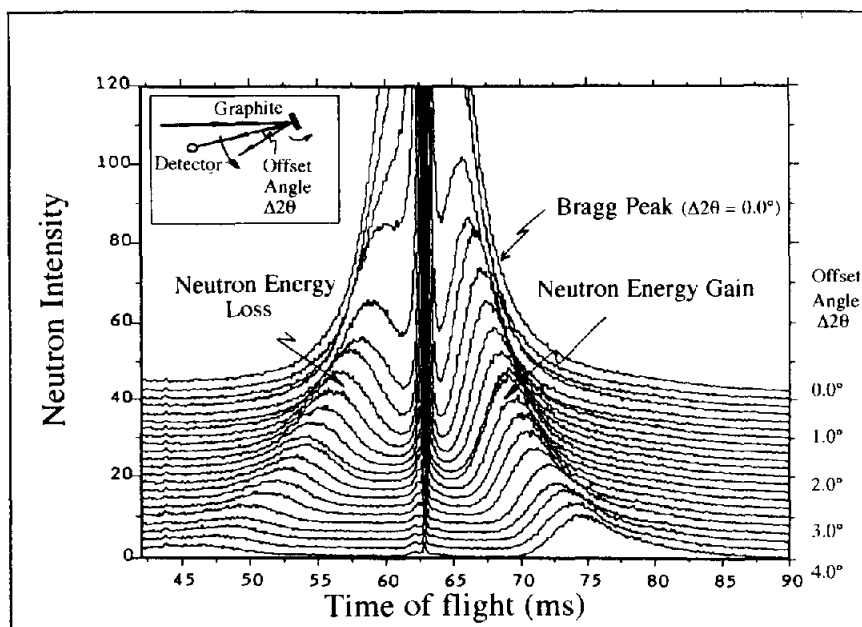


Fig. 7. The time-of-flight pattern of the (002) reflection from graphite recorded on the IRIS diffraction detector as a function of angular offset from the Bragg condition.

coarse collimator between the analyser and the detector but this would leave unaffected the most intense contribution to the TDS signal which lies at or close to the Bragg condition itself.

A second method, which has been adopted on IRIS, is to cool the analyser to attempt to reduce the effects of TDS. Tests were carried out on IRIS with the graphite crystal in a helium cryostat at the sample position and scattering patterns were recorded in the diffraction detector as a function of offset from the Bragg condition. In fig. 8 the patterns as a function of temperature are shown for an offset of  $4^\circ$  from the (002) reflection of graphite at a wavelength of  $6.6 \text{ \AA}$ . From the inset in fig. 8 the drop in TDS intensity is seen to be almost linear with the fall in temperature. Thus a graphite analyser operating at 25 K would be expected to produce a background from TDS sources which is an order of magnitude lower than for a room temperature analyser, with no loss in the elastic intensity. The elastic intensity itself is unaffected by the fall in temperature. The graphite analyser on IRIS has now been cooled to 25 K by a combination of

compressed-helium and liquid-nitrogen cooling circuits. The effect has been to improve the signal to background from a 1 mm plate sample of vanadium from 125-to-1 to 1350-to-1, more than a factor ten. This improvement in background is crucial in the reliable study of QENS and low intensity tunnelling lines.

#### 4.3. Optimisation of long-wavelength analysers

Mica is used as a generic term for the two-dimensionally layered aluminosilicate structural family existing in different chemical compositions with  $d$ -spacings from  $9 \text{ \AA}$  to  $11 \text{ \AA}$ . The (001) set of reflections from a mica single crystal in near backscattering geometry will therefore reflect monochromatic neutrons of wavelength  $20 \text{ \AA}$ ,  $10 \text{ \AA}$ ,  $6.7 \text{ \AA}$  etc. The diffraction pattern from muscovite 'amber' mica is shown in fig. 9 as a function of  $d$ -spacing. What is clear is that TDS is virtually absent from the (002), (004) and (008) reflections and very low on the (006) reflection. If we examine the individual line shapes from the mica analysers using vanadium as a scattering sample we can describe them by a

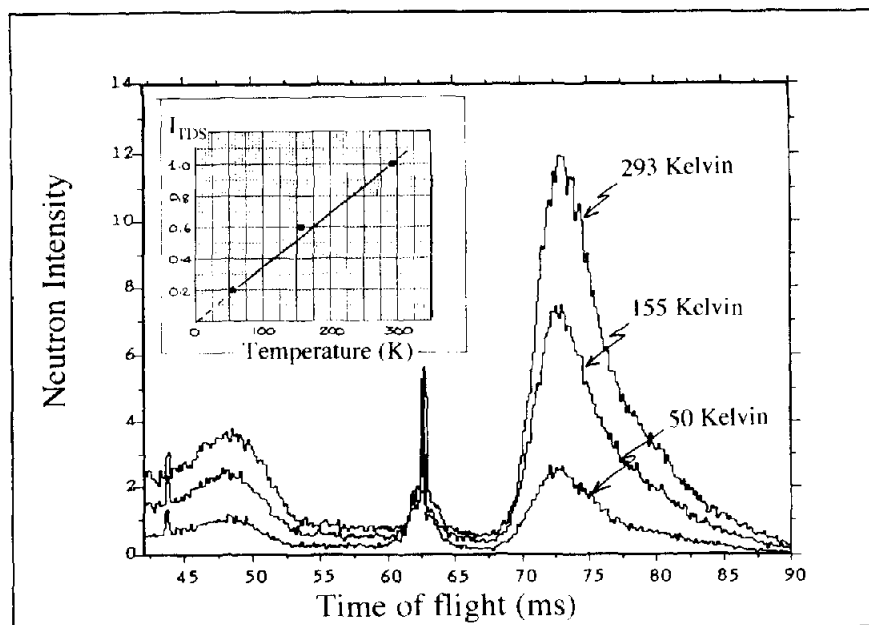


Fig. 8. The effect of cooling on the TDS close to the (002) reflection from graphite. The offset angle is  $4^\circ$ . The insert shows the integrated TDS intensity as a function of temperature.



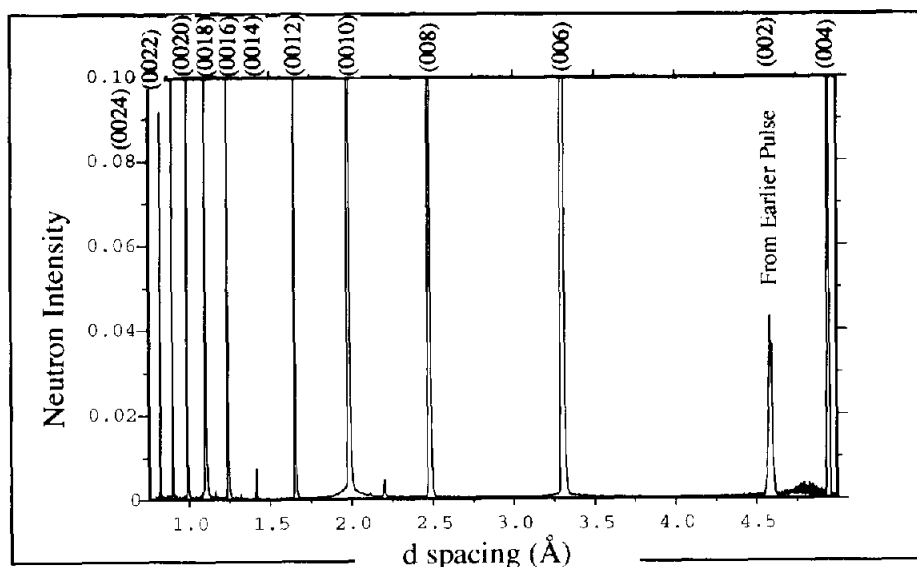


Fig. 9. The time-of-flight diffraction pattern of the (001) reflections from muscovite mica. The (0026) reflection is out of place due to frame wrap-around and the (002) reflection originates from an earlier ISIS pulse.

single gaussian convoluted with a decaying exponential and, more importantly, the rising edge is extremely sharp giving the opportunity of observing weak quasielastic scattering extremely clearly. The energy resolutions of the array of elastic lines from muscovite mica is shown in table 2.

The thickness of the IRIS mica analysers is 4 mm and the reflectivity of the (006) reflection is approximately 40% that of graphite. The 4 mm thickness is made up of approximately 12 sheets of varying thicknesses. Mica, as an analyser, offers great promise which has yet to be fully realised. Little is known about its neutron reflecting properties and more development work

Table 2

Resolutions of the (001) reflections from mica on IRIS using a vanadium sample.

Order	Analyser energy [meV]	Energy resolution [ $\mu$ eV]
(0010)	5.2	44
(008)	3.33	22
(006)	1.87	11
(004)	0.832	4.2
(002)	0.208	1.1

is required. The value for  $\Delta d/d$  for the various chemical isomorphs is unknown and the optimum thickness, maximum reflectivity and minimum background has not yet been explored. A full survey of the various varieties has yet to be carried out. Nevertheless it is clearly a material worthy of more study.

## 5. Future plans

Operational experience on pulsed sources in the past few years has put us in a strong position to capitalise on the advances achieved with the first-generation instruments and their developments. It is clear that high resolutions can be obtained quite readily on pulsed-source instruments with good intensities and that scientific advances follow such improvements in resolution. The copious fluxes of cold neutrons generated on pulsed sources has surprised even those people close to the moderator design and future instrumentation will exploit these cold neutrons. Equally well the original instruments were somewhat conservative being designed without the benefit of today's experience.

Therefore in laying down plans for future instruments the direction is clear. We must further improve resolution and range. The improvement of intensity, for its own sake, is of limited value.

Accordingly, plans have been drawn up to separate the high and medium resolution options of IRIS into two instruments on twin guide tubes from the same beam hole. OSIRIS will be a new spectrometer benefitting from experience gained on IRIS over the past four years which seeks to optimise the use of mica with resolutions improved by a factor of two and, by using very-large-area analysers, utilise to the full the plentiful supply of cold neutrons from the hydrogen moderator. IRIS, the original instrument, will then contain the cold graphite analysers, increased in area by a factor of three. The space released by the present mica analyser will be used to install a large position-sensitive diffraction detector for long  $d$ -spacing diffractometry using neutrons up to  $30 \text{ \AA}$  in wavelength with high intensities and a resolution  $\Delta d/d$  of  $2.5 \times 10^{-3}$ . Additional space in the tank will be used to install a prototype polarisation analysis set-up using a supermirror bender to polarise the inci-

dent beam and Heusler analysers for the scattered beam.

Backscattering crystal-analyser spectrometers on pulsed sources have come of age with the attainment of microvolt resolutions, the extension of the energy transfer ranges attainable with the best resolutions and, perhaps most surprisingly, when the accepted wisdom still persists in propagating the now outdated notion that pulsed sources are sources of epithermal neutrons only, good count rates even at wavelengths of  $20 \text{ \AA}$  and beyond.

## References

- [1] Instrumentation for Neutron Inelastic Scattering Research, in: Proceedings of a Panel held in Vienna, 1-5 December 1969, IAEA (1970) p. 35.
- [2] C.J. Carlile and J.S. Higgins, High Resolution Inelastic Spectrometers for SNS, RAL internal report, August 1976.
- [3] B.A. Dasannacharya, P.S. Goyal, C.L. Thaper, K.R. Rao, N.S. Satya Murthy and P.K. Iyengar,  $\Delta T$ -Window Spectrometer, BARC Trombay Report, July 1984.
- [4] B.T.M. Willis, C.J. Carlile, R.C. Ward, W.I.F. David and M.W. Johnson, *Europhys. Lett.* 2 (1986) 767.